Front. Struct. Civ. Eng. 2022, 16(2): 161–174
https://doi.org/10.1007/s11709-021-0796-7

RESEARCH ARTICLE

Enhancing compressive strength and durability of self-compacting concrete modified with controlled-burnt sugarcane bagasse ash-blended cements

Duc-Hien LE[a], Yeong-Nain SHEEN[b*], Khanh-Hung NGUYEN[c]

[a] *Sustainable Developments in Civil Engineering Research Group, Faculty of Civil Engineering, Ton Duc Thang University, Ho Chi Minh City 700000, Vietnam*

[b] *Department of Civil Engineering, Kaohsiung University of Science and Technology, Kaohsiung 80778, China*

[c] *Department of Civil Engineering, Lac Hong University, Bien Hoa 810000, Vietnam*

[*] *Corresponding author. E-mail: sheen@nkust.edu.tw*

ABSTRACT In sugar industries, the growing amount of sugarcane bagasse ash (SBA), a byproduct released after burning bagasse for producing electricity, is currently causing environmental pollution. The residual ash displays a pozzolanic potential; and hence, it has potential as a cement addictive. This study focuses on enhancing suitability of SBA through incorporating ground blast furnace slag (BFS) in manufacturing self-compacting concretes (SCCs). For this purpose, SBA was processed by burning at 700 °C for 1 h, before being ground to the cement fineness of 4010 cm^2/g. SCC mixtures were prepared by changing the proportions of SBA and BFS (i.e., 10%, 20%, and 30%) in blended systems; and their performance was investigated. Test results showed that the presence of amorphous silica was detected for the processed SBA, revealing that the strength activity index was above 80%. The compressive strength of SCC containing SBA (without BFS) could reach 98%−127% of that of the control; combination of SBA and 30% BFS gets a similar strength to the control after 28 d. Regarding durability, the 10%SBA + 30%BFS mix exhibited the lowest risk of corrosion. Moreover, the joint use of SBA and BFS enhanced significantly the SCC's sulfate resistance. Finally, a hyperbolic formula for interpolating the compressive strength of the SBA-based SCC was proposed and validated with error range estimated within ±10%.

KEYWORDS sugarcane bagasse ash, self-compacting concrete, compressive strength, sulfate resistance, water absorption, strength formula

1 Introduction

Self-compacting concrete (SCC) is one of the most popular concretes, firstly developed in the late 1980s in Japan, and recently popularly used worldwide due to its remarkable advantages. When compared with conventional concrete [1,2], it does not need additional vibrating or compacting works to obtain good concrete quality. In fresh state, SCC has the excellent ability to stream and compact itself using its own weight without segregating or bleeding. In addition, hardened SCC manifests high performance in terms of mechanical strength and durability regarding resistance against chloride diffusion, water absorption (*WA*), and permeability [2]. To ensure high fluidity besides good cohesiveness, the amount of Portland cement and fillers (passing through the 0.125 mm sieve, active or inert) of the SCC mixture must be significantly increased when compared to conventional concrete [1,3]. In addition, reduction of coarse aggregate content, and aggregate's maximum size together with new generation of super plasticizers (i.e., superplasticizers, viscosity-modifying agent) are required. Therefore, SCC is expensive, mainly due to the use of chemical admixtures and high volumes of Portland cement. A number of earlier scholars have demonstrated that mineral admixtures (i.e., fly ash (FA),

Article history: Received Aug 26, 2021; Accepted Nov 2, 2021

ground granulated blast furnace slag (BFS), silica fume, limestone powder) could be added to the mixture to improve SCC performance. It is well recognized that incorporation of slag or FA can beneficially increase the workability and long-term properties of concrete [4,5]. The utilization of these pozzolans becomes more effective, not only to reduce the manufacturing cost but also to enhance sustainability owing to high consumption of industrial by-products that may have no other use [1]. In recent years, it has been reported that agricultural ashes, generated from burning bio-wastes, such as rice husk, sugarcane bagasse, straw, seed shells, etc., can potentially be used as pozzolanic material to partially replace Portland cement in mortars and concretes, because they have a high content of bio-silica (SiO_2) [6–8]. In general, reactive silica in these ashes chemically reacts with calcium hydroxide, released during cement hydration, to form additional CSH gels, leading to improve concrete properties [9]. In the sugar industries, sugarcane bagasse ash (SBA), discharged after burning bagasse in cogeneration plants to produce electric power, is growingly dumped in free lands, causing environmental pollution [6]. The literature shows that after optimizing the processing methods, SBA can be used as a supplementary cementitious material (SCM) to improve the mechanical properties of concretes— including improvement of tensile strength, compressive strength, modulus of elasticity [10,11] and durability, increased chloride resistance [12], control of the alkali-silica reaction in reactive aggregate concrete [13], and reduction of the detrimental effect of sulfate attack [11,14]. However, raw SBA collected from specific sources is basically unfit for direct use in cementitious systems due to high content of unburnt coarse particles [15]. Large particle size with porosity of "as-received" SBA absorbs more water, which is unfavorable for performance of cementitious composites, especially in hardened state [16].

Calcination of raw SBA at a strictly controlled temperature combined, with grinding to the cement fineness (around 3000 cm^2/g, Blaine), was previously introduced to enhance its reactivity. Bahurudeen and Santhanam [15] studied re-burning SBA for 90 min at a temperature range of 600−900 °C, and identified that the highest pozzolanic activity was obtained at 700 °C using the strength activity index (SAI). Moreover, resistance to chloride ion penetration of concretes, incorporating with the treated SBA, increased by 2−3 times that of concrete with pure OPC at 28 and 90 d. Furthermore, Cordeiro and Kurtis [16] stated that increase of pozzolanic activity was associated with increasing fineness of ground SBA. A similar observation was also made by Cordeiro et al. [10]. Nevertheless, when SBA has a very high content loss following combustion, sole grinding may be inefficient. On the other hand, Zareei et al. [17] reported a different behavior in ordinary and SCCproduced with 5%−25% ordinary Portland cement (OPC) replaced by equivalent proportions of SBA and processed by re-burning at 700 °C for 1 h before cooling to room temperature. Their results displayed that increase in SBA replacement resulted in decreasing mechanical strength of the concretes, due to low pozzolanic activity of the cementing replacement additive. In spite of that, incorporation of SBA improved the durability and other qualities of SCC such as increase in passing and flowability, and increase in impact resistance together with decrease in *WA*. It is therefore noticed that individual sources of SBA must be examined in terms of chemical and physical characteristics before use, from which the most effective utilization of the bio-waste is determined [18].

This study focuses on enhancing suitability of SBA through incorporating ground BFS in manufacturing SCCs. The presence of slag in the ternary binder is expected to counteract the negative effect of SBA, and further reduces the amount of OPC used thus achieving greater sustainability. The studies on this subject are few. For this purpose, SBA collected from a specific source near a sugar factory was processed by burning in a muffle furnace at 700 °C for 1 h and grinding to the cement fineness before being used as a SCM. Physical and chemical characteristics of the resulting ash were examined to confirm effectiveness of the pre-treatment of SBA. Moreover, influences of SBA in combination with slag on the properties of ternary-blended SCCs were investigated.

2 Experimental plan

2.1 Materials used

Type I OPC, ground granulated BFS, Type F FA, processed-sugarcane bagasse ash (P-SBA), crushed stone, river sand, superplasticizer and tap water are primary materials used in the preparation of SCC mixtures.

1) OPC, BFS, FA: OPC Type I/PCB40, conforming to the ASTM C150 [19] was used. The specific Blaine fineness of the cement is 3530 cm^2/g; and its relative specific gravity is 3.15. Besides, commercial slag Grade 80 and FA Type F (ASTM C618), collected from a cement plant, were used in developing SCC mixtures. Properties of these materials are presented in Tables 1 and 2.

2) SBA: Bagasse ash used in this investigation was collected at random from an opened dump nearby a local sugar factory. The collected bagasse ash was dried at 110 °C for 24 h to remove free water and before sieving through the No.50 sieve (opening of 323 μm) to eliminate unburnt coarse substances. The sieved ash was re-calcined by strictly burning in a muffle furnace at

Table 1 Oxides composition for OPC, BFS, FA, and P-SBA used in this study

material	oxides content (%)										LOI*(%)
	SiO_2	Al_2O_3	Fe_2O_3	CaO	MgO	SiO_3	P_2O_5	MnO_2	Na_2O	K_2O	
OPC	20.8	4.7	3.13	63.2	3.33	2.01	–	–	0.21	0.51	2.11
BFS	36.61	12.92	0.37	42.1	6.6	0.51	–	–	–	–	0.89
FA	46.01	37.21	4.69	2.88	1.99	0.71	–	–	0.22	1.16	5.13
P-SBA	53.2	6.89	3.00	3.451	2.82	–	–	–	0.662	7.076	14.3

*Note: LOI, Loss on ignition.

Table 2 Physical properties of OPC, BFS, FA, and P-SBA used in this study

physical property	OPC	BFS	FA	P-SBA
specific gravity (g/cm^3)	3.15	2.8	2.2	2.02
fineness (g/cm^2)	3530	4550	4050	4010
water consistency (%)	28	–	–	55
SAI as per ASTM C311				
+ SAI at 7 d (%)	–	–	–	83.40
+ SAI at 28 d (%)	–	–	–	84.66

700 °C for 1 h, followed by a fast cooling down to room temperature. Then, it was ground with a ball mill to decrease its particle sizes to the cement fineness greater than approximately 3500 cm^2/g). The resulting ash (processed ash, denoted as P-SBA thereafter) was stored in air-tight plastic bags for the experiment. The P-SBA sample was characterized by its chemical and physical characteristics. The oxides contents of P-SBA sample were determined using X-ray fluorescence (XRF) technique; the morphology of the same ash was detected by Scanning Electric Microscope (SEM); X-ray diffraction (XRD) examination of P-SBA was also carried out.

3) Aggregates: Coarse aggregate (C/A) was produced from crushed stone with the fineness modulus (F.M) of 6.22; it has the *WA* value of 2.45%, and relative gravity of 2.65. Fine aggregate (F/A), sourced from river sand has the F.M value of 2.87, the WA value of 1.66% and relative density of 2.64. Both aggregates (coarse and fine) used in this investigation fully conformed to the ASTM C33 [20] for making concrete.

4) Chemical admixture: A Polycarboxylate-based superplasticizer (SP), complying with ASTM C494 Type F, with the density of 1.06−1.09 g/cm^3 (at the temperature of 20 °C), pH of 6, and concentration of 14%−22% was used to improve workability of SCC mixtures.

2.2 Mix proportions for blended cementing SCCs

The SCC mixtures in this study were designated using a densified mixture design algorithm (DMDA) approach, proposed in earlier publication [21]. The concept of the DMDA follows the assumption that the best concrete performance could be achieved when its density is high. The DMDA mixture was incorporated with FA to fill the voids among aggregates as much as possible, effectively increasing the density of the aggregate system. In this case, FA plays roles of filler (physical effect) as well as pozzolanic material (chemical effect). Moreover, in the proposed SCC mixtures, OPC was partially replaced by P-SBA and BFS in order to fabricate the binary (OPC + SBA) and ternary (OPC + SBA + BFS)–blended cements. The water-powder ratio (*w*/*p*) was fixed at 0.45 after several trials; and water-reducing agent with a dosage of 1.4% weight of powder was added to achieve the target workability. In summary, 13 mix proportions were prepared for the experimental program, as shown in Table 3.

2.3 Testing items of SCCs

2.3.1 Fresh state tests

The slump flow, box-filling height, T-500 (time for reaching flow diameter of 500 mm), and V-funnel tests were carried out in accordance with Japan Society of Civil Engineering (JSCE) [22] specifications to investigate the influences of cement replacement materials on the SCC characteristics in fresh state.

2.3.2 Hardened state tests

Table 4 briefly describes the ASTM testing procedures adopted for investigating performance of the SCCs at different periods. Accordingly, compressive strength, *WA*, electrical resistivity (*ER*), and resistance to sulfate attack tests were included. The fresh SCC mixtures, after measurement of slump flow, were freely poured into cylindrical steel modes with a dimension of 100 mm in diameter and 200 mm in height; the SCC samples were self-compacted well without any need of compacting/vibrating work due to their own weight. After 24 h of casting, the specimens (273 specimens in total, see Table 4) were removed from the molds and submerged in water tanks for curing until the testing age was reached. In this study, each testing result was triplicated, and the average values from three identical specimens were reported.

Table 3 Mix proportion for 1 m^3 of SCC

No.	mix ID	*w*/*p*	binder proportion (%)			FA (kg/m^3)	aggregates (kg/m^3)		SP (%)
			OPC	SBA	BFS		C/A	F/A	
1	control	0.45	100	–	–	124	811	828	1.4
2	10SBA		90	10	–				
3	20SBA		80	20	–				
4	30SBA		70	30	–				
5	10SBA + 10BFS		80	10	10				
6	10SBA + 20BFS		70	10	20				
7	10SBA + 30BFS		60	10	30				
8	20SBA + 10BFS		70	20	10				
9	20SBA + 20BFS		60	20	20				
10	20SBA + 30BFS		50	20	30				
11	30SBA + 10BFS		60	30	10				
12	30SBA + 20BFS		50	30	20				
13	30SBA + 30BFS		40	30	30				

Notes: *w*/*p* denotes the water-powder ratio; powder content = (OPC+SBA+BFS+FA); SBA indicates processed bagasse ash (P-SBA); C/A and F/A denote the coarse and fine aggregates, respectively.

Table 4 Testing items for hardened SCCs

testing item for SCCs and associated ASTM standards	testing age	No. of cylindrical specimens (100 mm in diameter × 200 mm in height)
compressive strength (ASTM C39)	7, 28, 56, and 91 d	12 × 13 = 156
WA (ASTM C642)		3 × 13 = 39
resistivity (ASTM WK37880)		3 × 13 = 39
sulfate resistance (ASTM C1102)	28 d	3 × 13 = 39
total	–	273

3 Results and discussion

3.1 Characterization of the P-SBA sample

Table 1 shows the oxides content of P-SBA sample, determined by XRF, in comparison with those of others (OPC, BFS, and FA). The analysis data presents that the highest silica (SiO_2) content was detected for the bagasse ash sample (53.2%), followed by FA (46.01%), and BFS (36.61%). The sum of pozzolanic oxides (SiO_2 + Al_2O_3 + CaO) of SBA was 63%, which was somewhat lower than the limitation of 70% for a pozzolan, recommended by ASTM C618 [23]. In addition, loss on ignition (LOI) of the P-SBA was extremely high (14.3%, which was reduced from 22.9% for the raw SBA). Previous investigations of SBA from many sources have shown that the LOI of untreated bagasse ash is remarkably high (greater than 10%, or even 20%), which is attributed to the unburnt fractions [15,24,25].

Moreover, photos of the SBA samples before and after re-calcining are shown Figs. 1(a) and 1(b). Due to presence of high carbon content, the raw SBA sample is black color, while the reddish-grey color is observed for the burnt sample, associated with reduction of LOI. A SEM image and XRD pattern of the burnt SBA sample are displayed in Figs. 1(c) and 1(d). More porous particles with a majority of prismatic sharps (marked-1) and a minor number of spherical sharps (marked-2) were detected for the P-SBA sample, indicating that this material tends to absorb more free water. Consequently, cementitious mixtures incorporated with the P-SBA will have greater water demand. In addition, XRD examination revealed an amorphous silica characteristic with traces of low quartz (α-SiO_2) and cristobalite (β-SiO_2) for the P-SBA sample. There is evidence that a broad hump, located at between 20°−30° (2θ angle) and seen on the spectra, suggested a silica-reactive material. Furthermore, several physical properties of P-SBA are reported in Table 2. Its Blaine fineness was determined to be 4010 cm^2/g (and those of OPC and BFS were found to be 3550 and 4550 cm^2/g, respectively). The relative specific density of P-SBA was 2.02, lower than that of both OPC (3.15) and BFS (2.80). Furthermore, the P-SBA's mortar SAI, determined in accordance to ASTM C311 [26], was 83.40% and 84.66%, evaluated at 7 and 28 d,

respectively. A pozzolan must ensure the SAI value is above 75%, required by ASTM C618; therefore, the P-SBA in this investigation fulfilled the requirement of a cementitious material in terms of strength contribution.

3.2 Fresh properties of blended SCCs containing SBA and BFS

Measurements of fresh properties of various blended-cementing SCCs including slump flow, filling-height, V-funnel flow time, T-500 time are reported in Table 5. By comparing the obtained results to the JSCE acceptance values, it can be seen that SCC mixtures containing SBA and BFS satisfied well the Class 2 filling ability, regarding the flowability and viscosity. For instance, the slump flow diameters were measured in range of 550−700 mm; the T-500 time and V-funnel flow time were between 4−9 and 9−16 s, respectively. In this work, all SCC mixtures in fresh state showed excellent fluidity with homogeneity; no bleeding or segregation was observed. Meanwhile, only 5/13 mixtures (i.e., control, 10SBA, 20SBA, 10SBA + 10BFS, 10SBA + 20BFS) had the filling-height values above 300 mm, conforming to the requirement of passing ability through the reinforcing gaps. The others (7 mixtures) might be not adequate for areas with highly congested reinforcements. Table 5 indicates that incorporating with SBA or with blends of SBA and BFS resulted in loss of flowability and passing ability of SCCs (less compatibility). Previous researchers have revealed that SBA dosage had a great impact on water demand of cementitious systems resulting from the hydrophilic nature of the cement replacement material [6,27]. In addition, angularity and irregular shape with rough surface of SBA and BFS particles would be attributed to workability loss because they will uptake water inside themselves [28,29]. Further differences in water demand may be because the specific gravity of SBA (2.02) is lower than that of OPC (3.15). As a result, a higher volume of SBA, than that of OPC, is required for the same weight replacement, leading to increased lubrication [18]. Furthermore, the flow times (via T-500 and V-funnel tests) were increased with greater addition of pozzolanic materials, showing more viscosity of the blended composites. Previous study on fresh SCC containing SBA showed similar observation [30].

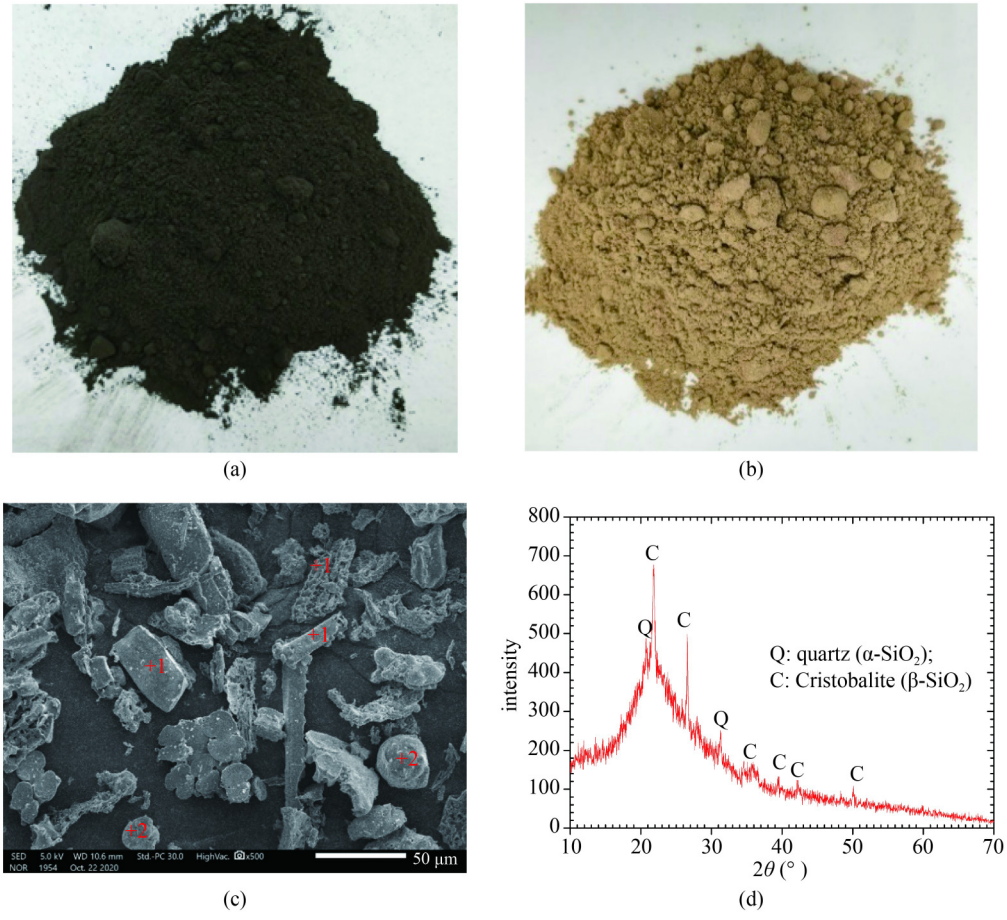

Fig. 1 Photos of SBA samples. (a) Raw SBA; (b) P-SBA; (c) SEM image of P-SBA sample; (d) XRD pattern for P-SBA used in this study. (+1): Prismatic particles with cell structure; (+2): Spherical molten amorphous silica.

Table 5 Fresh properties of blended SCCs in this investigation

No.	mix ID.	slump flow (mm)	box-filling height for gaps (mm)	T-500 time (s)	V-funnel flow time (s)
1	control	671	330	4.2	9.0
2	10SBA	625	312	5.5	9.5
3	20SBA	611	302	6.4	10.4
4	30SBA	584	286	7.1	12.9
5	10SBA + 10BFS	650	310	5.3	10.4
6	10SBA + 20BFS	637	300	6.3	11.3
7	10SBA + 30BFS	611	291	6.4	12.1
8	20SBA + 10BFS	623	291	5.9	11.2
9	20SBA + 20BFS	612	280	6.5	12.5
10	20SBA + 30BFS	586	272	7.1	14.1
11	30SBA + 10BFS	591	274	6.8	13.5
12	30SBA + 20BFS	573	260	7.7	14.3
13	30SBA + 30BFS	551	244	8.9	15.8
accepted range according to JSCE	–	500–750	⩾ 300	3–20	7–20

3.3 Compressive strength of blended SCCs containing SBA and BFS

The results of compressive strength test at different periods (i.e., 7, 28, 56, and 91 d) of the SBA-blended concrete (with and without BFS) and control concrete are displayed in Fig. 2. The figure shows that the compressive strength was progressively developed over time as a result of the hydration and pozzolanic reactions. It is noticed that, at early age (7 d), the mixtures 30SBA + 10BFS, 30SBA + 20BFS and 30SBA + 30BFS were not yet sufficiently solidified, and their strength values were lower than those of the others. Thus, addition of BFS in SCCs containing 30%SBA is inappropriate, in terms of compressive strength, only at early ages. This result may be due to slow reaction of the cement substitutes when their dosages were high (40%–60%). With the exception of these mixtures, the strength ratios between 7 and 28 d ($f_{c,7}/f_{c,28}$) for other SCCs were evaluated around 0.73–0.81; and the strength ratios were in range of 1.05–1.12 when the strengths at 91 and 28 d were compared. There was a slight improvement of compressive strength along with the increase in replacement percentage of SBA for OPC at all testing ages. The control SCC with pure OPC had compressive strengths of 21.2, 32.1, 34.6, and 35.2 MPa, determined at 7, 28, 56, and 91 d, respectively; the compressive strength of SBA cementing concrete (without BFS) was superior to that of the respective controls. For instance, at 28 d, the strength of SCCs fabricated with 10%, 20%, and 30% bagasse ash reached 98%, 127%, and 104% that of the control, respectively; at 91 d, the corresponding strengths of 98%, 106%, and 108% were estimated. Previous researchers [11,31] found that concrete modified with an appropriate quantity of SBA replacing OPC could clearly improve the mechanical strength. The increase in strength compared to the control could be attributed to pozzolanic reaction, in which reactive silica component in the SBA reacts with $Ca(OH)_2$ (from hydration of OPC) to additionally form CSH gels. Moreover, filler effect of finer SBA particles, which physically fill the voids in the cement matrix and increase the density, resulted in additional strength gained [11]. However, when SBA excessively increased, the strength drop was seem to be likely to occur due to the lower OPC content [6]. On the other hand, SCC that incorporated both SBA and BFS to partially replace OPC (ternary-blended system) had the strength higher than that of the control at early age (7 d), with the exception of the 30SBA series (+ 10BFS; + 20BFS; and + 30BFS). However, this trend reversed as the curing age extended to 28 d or longer. Ternary cementing concrete experienced a substantial strength reduction at later ages (28–91 d), when compared to the control SCC and to the respective binary cementing SCC, although increasing BFS in the mixtures led to improvement of the strength. The higher strength at early age (7 d) and lower strength at later age of ternary composites than those of the control may be attributed to the higher *WA* of both of the cementing alternatives, inducing more porosity within the mentioned concrete [32]. In addition, it was observed that 30% BFS in the ternary blended system presented a comparable strength of the control after 28 d. For example, SCC specimens made from mixtures of 10SBA + 30BFS, 20SBA + 30BFS, 30SBA + 30BFS achieved a strength level of 95%–101% relative to the control, tested at 28 and 91 d. The reasons might be due to filling the empty spaces with finer inclusions (physical effect) and consuming $Ca(OH)_2$ during hydration of OPC (pozzolanic effect). Study on the ternary concretes containing SBA (sieving through a No. 75 μm filter) and FA also

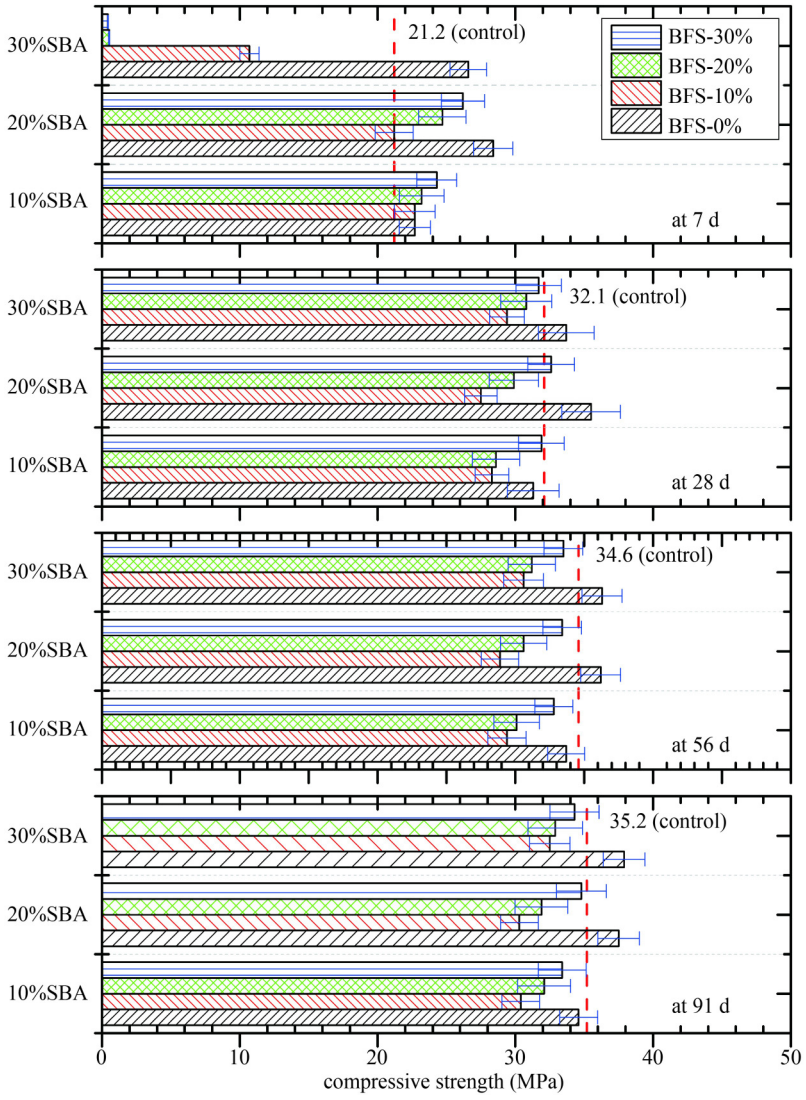

Fig. 2 The results of compressive strength test for all SCC mixtures.

reported a similar observation [33]. Based on the obtained results, the combination of 30SBA + 30BFS could be optimum, because it took the lowest OPC content (and highest cement replacement used) and attained a comparable compressive strength of the control.

3.4 Electrical resistivity of blended SCCs

The measurement results of *ER* of different SCC mixtures at various ages (7, 28, 56, and 91 d) are reported in Table 6. It can be seen that resistivity of the SCC specimens was growing over aging times, owning to gradual reduction of porosity with hydration products. After 28 d, the *ER*-values of the SCC specimens were mostly above the limitation of corrosive prevention (20 kΩ·cm), recommended by CEB-192 [34], with the exception of the mix 30SBA + 30BFS (13.5 kΩ·cm). Increasing rates of SBA replacement for OPC in the binary-blended cement led to a gradual decrease of resistivity at the later ages. For example, in this study, when 10%, 20%, and 30% SBA were incorporated, the *ER*-value was decreased by 5%, 11%, and 24%, respectively, relative to the control, evaluated at 91 d. In general, *ER* is closely related to the pore structure and pore solution features (ion penetrability) within concrete [35]. Rukzon and Chindaprasirt [36] examined the influence of SBA as cement replacement on the porosity of concrete and concluded that the higher the SBA dosage that replaced OPC the higher the porosity of the concrete. The authors evidenced that porosity of control concrete at 28 d was 7.2%; and that values for blended concrete prepared with 10%, 20%, 30%SBA replacement were 7.22%, 8.31%, and 8.50%, respectively. This seems that the larger amount of SBA substituted for OPC caused insufficient reaction of $Ca(OH)_2$ (from cement hydration) with silica from the bagasse ash, which could be attributed to the porosity increase, which in turn affected the resistivity directly [11]. Further, among the ternary-blended SCCs, the mix 10SBA + 30BFS showed the highest resistivity after 28 d, which was slightly higher than that of the

control, and it therefore exhibited the lowest risk of corrosion. This is remarkable evidence for effective pore-structure refinement of the mentioned combination.

3.5 Water absorption of blended SCCs

The measurement results of *WA* are tabulated in Table 7. The measured data expressed an essential trend of larger decrease of *WA*, along with the prolonged aging, related to the formation of hydration products, resulted in reduction of porosity of concrete structure. Hence, the lowering *WA* was generally associated with increase of mechanical strength, as discussed previously. For binary-blended cement SCC, at later ages (after 28 d), percentage mass of absorbed water was increased with the larger amount of SBA replacement. Mixtures containing 10%, 20%, and 30% SBA had the *WA* values of 3.77%, 3.78%, and 4.68%, respectively, which were higher than those of controls determined at 28 d (2.11%); in addition, the increasing rate of *WA* was significant at 28 d and it gradually reduced at 56 and 91 d. This result was in agreement with those of earlier authors [37,38]. Larger specific surface area (finer particles) was the case for OPC, and hygroscopic nature of SBA, which tends to absorb more mixing water, would be responsible for the mentioned behavior.

Table 6 Results of *ER* of different SCCs

No.	mix ID	*ER* (kΩ·cm)			
		7 d	28 d	56 d	91 d
1	control	11.00	31.25	57.75	98.25
2	10SBA	10.00	32.00	55.00	93.25
3	20SBA	9.06	31.25	53.25	87.25
4	30SBA	7.90	26.00	46.75	74.25
5	10SBA + 10BFS	7.53	29.00	51.50	85.75
6	10SBA + 20BFS	8.35	34.50	56.75	87.75
7	10SBA + 30BFS	9.35	36.25	67.75	98.50
8	20SBA + 10BFS	7.40	31.00	50.75	79.25
9	20SBA + 20BFS	7.50	32.75	53.00	81.75
10	20SBA + 30BFS	7.85	30.15	58.50	88.25
11	30SBA + 10BFS	5.67	28.00	48.50	79.25
12	30SBA + 20BFS	4.58	21.00	41.75	67.25
13	30SBA + 30BFS	4.20	13.50	38.75	65.25

Table 7 Results of *WA* of SCCs and weight loss of different SCCs

No.	mix ID	*WA* (%)				weight loss (%)
		7 d	28 d	56 d	91 d	
1	control	2.62	2.11	2.08	2.07	2.52
2	10SBA	3.49	3.77	2.88	2.20	2.06
3	20SBA	3.06	3.78	3.13	2.16	2.00
4	30SBA	3.92	4.68	3.75	2.74	1.83
5	10SBA + 10BFS	3.46	4.03	3.24	2.89	1.49
6	10SBA + 20BFS	3.11	3.98	3.08	2.51	1.13
7	10SBA + 30BFS	2.63	3.24	2.88	2.30	1.13
8	20SBA + 10BFS	4.31	5.21	4.58	3.66	0.83
9	20SBA + 20BFS	4.47	4.48	3.69	3.36	0.61
10	20SBA + 30BFS	3.79	3.84	3.23	3.03	0.49
11	30SBA + 10BFS	4.72	6.72	5.14	4.11	0.37
12	30SBA + 20BFS	5.06	6.07	4.83	3.23	0.18
13	30SBA + 30BFS	5.25	5.57	3.76	3.21	0.18

In addition, increasingly adding BFS to the binary cement system containing SBA led to steady reduction of *WA* in the SCC samples at later ages. In particular, at 91 d, the *WA*-values of the 10SBA mix series combined with 10%, 20%, 30%BFS were 2.89%, 2.51%, and 2.30%, respectively. Other mix series also had a similar trend. However, SCC containing both SBA and BFS had the *WA*-value higher than that of the respective control, measured at the same condition. The fact seems due to lack of the required amount of calcium hydroxide, which released during cement hydration, to react with amorphous silica in the replacement materials. The consequence of unavailability of $Ca(OH)_2$ at the nucleation sites would be reduced in formation of CSH gels, resulting in more porosity and water retention in the saturated condition [11]. Furthermore, Fig. 3 depicts the experimental relationships between *WA* versus *ER* at different curing ages. The plot showed a trend that the higher *WA* the lower the observed resistivity, resulting from the fact that the two mentioned-durability indices are physically related to liquid accessible porosity of concrete [39]. As seen in the figure, the *WA*−*ER* correlations for each aging time can be expressed by a power formula ($ER = a \times WA^{-b}$); where a and b are constants, obtained through regression analysis of the testing data. An analogous relationship between the two indices can be found in the previous study [35].

3.6 Weight loss of blended SCCs due to immersion in a 5% sodium sulfate solution

The results of weight loss for different SCC specimens due to exposure in sulfate solution are presented in Table 7. It can be observed that the loss of weight for control SCC was highest, calculated at 2.52%, manifested the highest level of degradation among different SCC specimens. In general, when immersed in sulfate environment, concrete sample is subject to degradation and weight loss, caused by expansion volume of cracks in cement paste. Nevertheless, replacing a part of OPC by SBA or by both SBA and BFS greatly enhanced the sulfate resistance, related to the fact that blended-cementing SCCs showed a lesser weight loss compared to the that of control SCCs with pure OPC. Also, increasingly higher SBA dosage in the binary binder (OPC + SBA) produced a lesser weight loss of SCC specimens, when immersed in aggressive media. The measured weight loss of 30SBA mix was 1.83%, which was decreased by 27.4% relative to the control mix. Interestingly, SCCs made with ternary-blended cement (OPC + SBA + BFS) performed with excellent sulfate resistance. The lowest loss of weight was obtained for the two mixes 30SBA + 20BFS (0.18%) and 30SBA + 20BFS (0.18%), followed by the mix series 20SBA (0.49%−0.83%) and 10SBA (1.13%−1.49%). Thus, it can be revealed that the higher the level of replacement of OPC by SBA and/or BFS the lower the weight loss was. The improvement of sulfate resistance in this study is in agreement with that reported in Refs. [1,14]. The reason may be due to concrete modification with pozzolanic materials basically resulted in less tricalcium aluminate (C_3A) and $Ca(OH)_2$ when compared to OPC concrete, which produced less ettringite and gypsum [14].

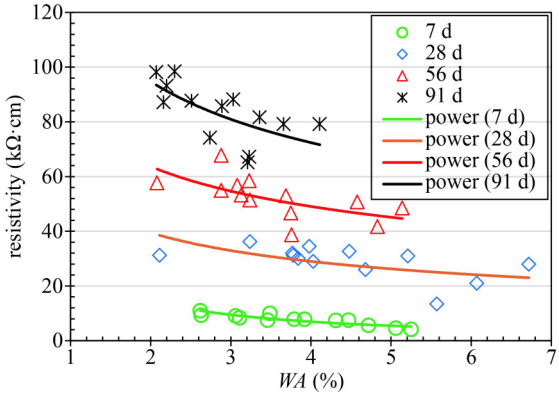

Fig. 3 Correlations between *WA* and *ER*.

3.7 Strength formulation for SBA-blended SCCs and validation

In this section, a strength formulation of the SBA-based SCCs is established. The ACI Committee 209 [40] recommends a hyperbolic formula (see Eq. (1)), which allows prediction of the compressive strength of a conventional concrete at a specific age, based on its corresponding strength determined at 28 d:

$$f_{c,t} = f_{c,28}\frac{t}{a+bt}, \quad (1)$$

where t is the curing age (d); $f_{c,t}$ and $f_{c,28}$ represent the compressive strengths of concrete at the ages of t and 28 d, respectively; a and b are coefficients of the hyperbolic function, with values of 4.0 and 0.85 (for normal concrete), respectively.

Wang et al. [41] revealed that with addition of additives such as slag, FA, waste glass in concrete mixtures, the trend of strength development over time for blended concrete was similar to that of conventional OPC, complying to the hyperbolic form, in spite of significant difference in the hydration rate of pozzolanic additives. In this study, based on the data set of compressive strength measured at different periods (7, 28, 51, and 91 d), adjustment of the coefficients a and b will be proposed for the SBA-based cementing SCCs using an analytical approach. By transforming Eq. (1), a linear formula of strength ratio between 28 d and t d (denoted as $f_{c,28}/f_{c,t}$) versus t^{-1} is obtained, as shown in Eq. (2):

$$\frac{f_{c,28}}{f_{c,t}} = \frac{a+bt}{t} = \frac{a}{t} + b = a \cdot t^{-1} + b. \quad (2)$$

Table 8 reports the values of a and b coefficients, which were determined from the regression analysis of the testing data (the trending lines). Also, Figs. 4 and 5 demonstrate the influences of SBA and BFS ratios on the two coefficients (i.e., a and b). A trend can be observed whereby the coefficient a decreased with an increase in SBA replacement ratio; BFS seems to have a minor impact on this coefficient. Meanwhile, both SBA and BFS ratios did produce a slight effect on the coefficient b (see Fig. 5). Based on this behavior, for simplicity, it could be assumed that the a-coefficient is a function of the SBA ratio only; whereas, the b-coefficient is not affected by both SBA and BFS replacement, meaning that it would take the value of 0.8474 for the control SCC with pure OPC (see Table 8). Regression analysis of the testing results for the SBA series (without BFS) shows that the a–coefficient and SBA rate (denoted as SBA in the formulae below) were correlated well (coefficient of determination, R^2 =0.75, see Fig. 4) with a linear trend, as Eq. (3):

$$a = -7.0357 \times SBA + 4.3647. \quad (3)$$

Finally,

$$f_{c,t} = f_{c,28} \times \frac{t}{-7.0357 \times SBA + 4.3647 + 0.8474 \times t}. \quad (4)$$

The comparison of actual (experimental) and calculated strength values from Eq. (4) is graphically illustrated in Fig. 6. The scatter plot indicates that, except for unexpected strength at early age for mixtures containing high dosage of cement replacement (30SBA series at 7 d), most of the data points, whose coordinates are the actual and calculated strengths, are closed to the bi-sector line (1:1 line), within the error range of ±10%. This description means that the calculated strengths interpolated from the analytical formula are closely comparable to the actual strength. The relative strength ($f_{c,t}/f_{c,28}$) evolutions over ages, obtained from the experiment and

Table 8 Coefficients a and b taken from regression analysis (the trending lines)

SBA (%)	BFS (%)			
	0	10	20	30
0 (control)	4.6486 [0.8474][a)]	–	–	–
10	3.5887 [0.8670]	2.3351 [0.9140]	2.4043 [0.8938]	2.7472 [0.9176]
20	2.2509 [0.9276]	2.8560 [0.8910]	1.9791 [0.9286]	2.2544 [0.9224]
30	2.7493 [0.8786]	N/A[b)]	N/A	N/A

Notes: a) The b-coefficient is placed in the square bracket [−]; b) the N/A indicates not available values due to unstable strength at 7 d.

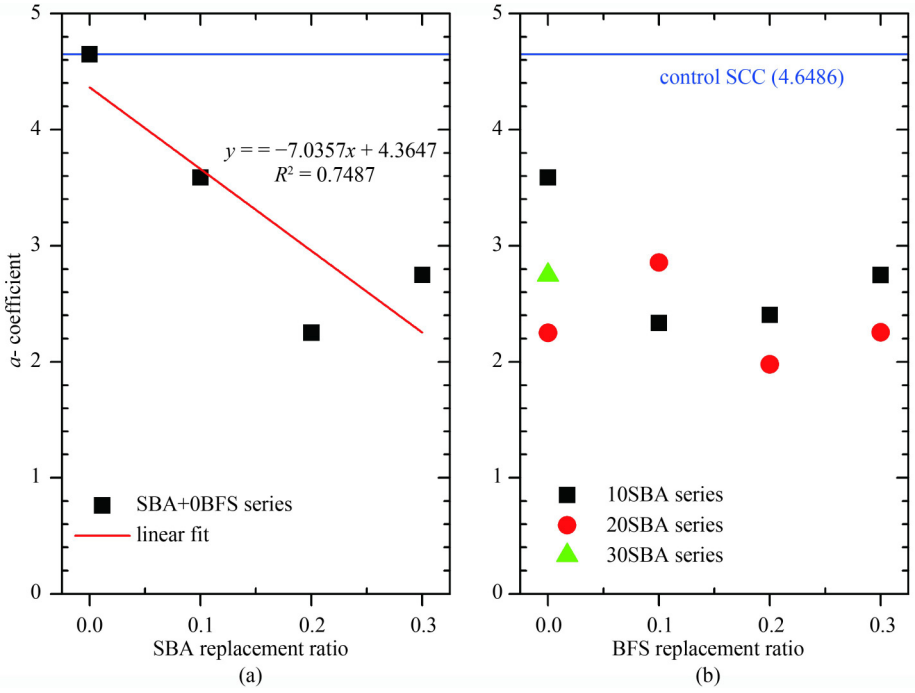

Fig. 4 Variations of a-coefficient versus (a) SBA and (b) BFS replacement ratios.

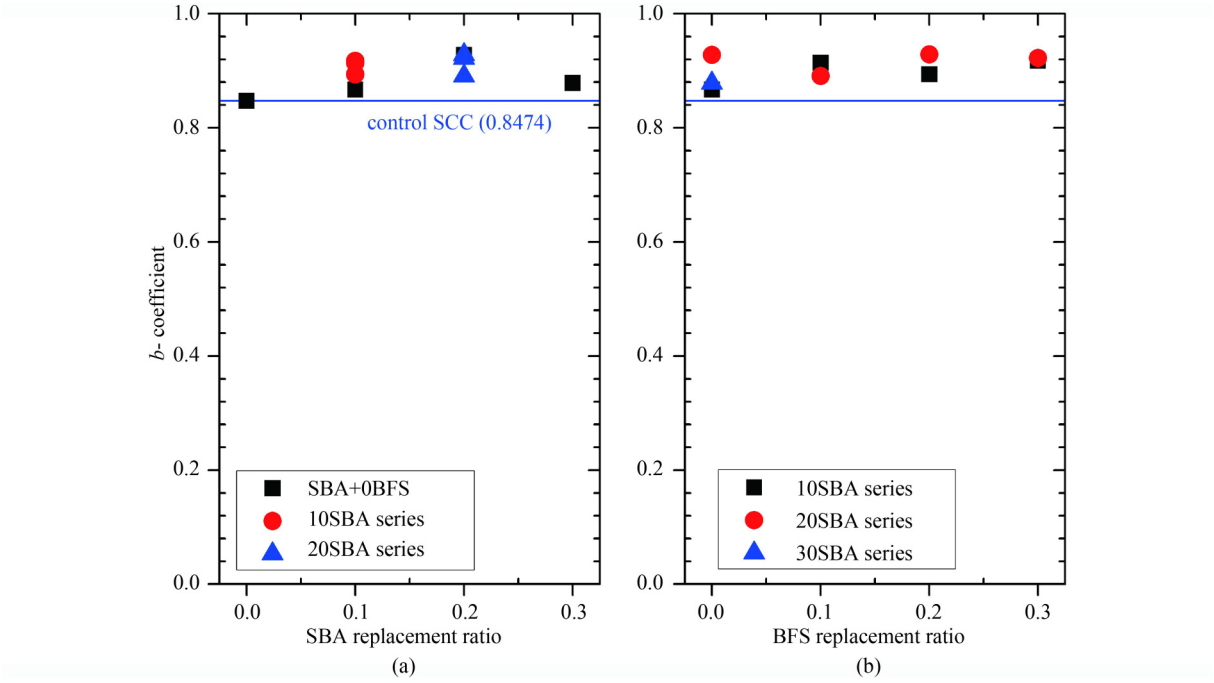

Fig. 5 Variations of *b*-coefficient versus (a) SBA and (b) BFS replacement ratios.

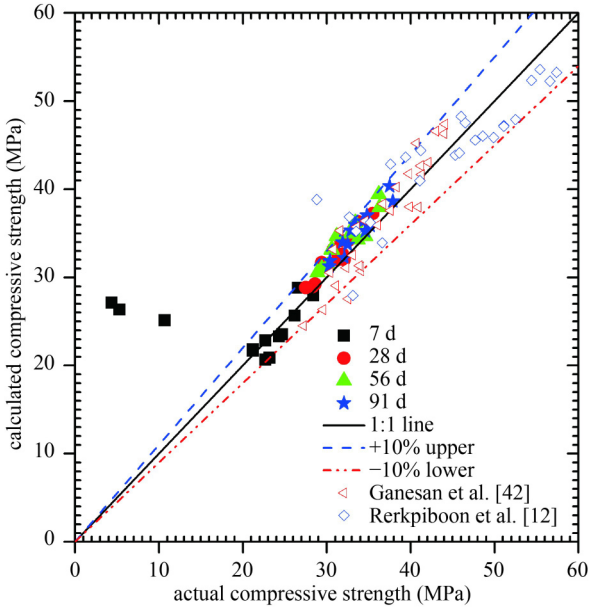

Fig. 6 Comparision of actual and calculated compressive strength.

from the interpolation for the SBA-based SCC, are comparably illustrated in Fig. 7.

Validation of the proposed formula. In addition, validation of the formula established in this study was carried out to check its efficiency. The testing data sets, previously published by Ganesan et al. [42] and Rerkpiboon et al. [12], were referred for validation. In accodance to these authors, concrete mixtures were prepared with SBA replaced for OPC at various ratios (i.e., 0.0−0.5); and the conpressive strengths of these concretes were experimentally determined at the aging times between 7 and 180 d. In Table 9, the compressive strengths interpolated from the proposed formula ($f_{c,cal.}$) are comprared to those collected in the literature ($f_{c,act.}$); the differences (errors, in percent) between them are also reported therein. Performance of the established formula was quantatively evaluated based on the MAPE (mean absolute percentage error) index, determined by the following Eq. (5):

$$MAPE, \% = \frac{1}{N} \times \sum_{i=1}^{N} \left| \frac{t_i - z_i}{t_i} \right| \times 100, \quad (5)$$

where t_i and z_i are the actual and interpolated values, respectively; N is the number of data points.

As seen in Tables 9 and 10, the *MAPE* values were 7.88% and 6.12% for the two validated sets. It is widely agreed that a *MAPE* less than 10% indicates an excellent interpolating ability [41]. From this viewpoint, the compressive strength values introduced from the proposed formula were highly reasonable, approximating well to actual values. Moreover, this statement was futher supported by the fact that most of the points showing the actual and calculated strengths are located near the bisector region (within error range of ±10%), as plotted in Fig. 6. Therefore, based on above analysis, the formula in the Eq. (4) is valid for interpolating the compressive strengths of different concretes containing SBA as cement replacement.

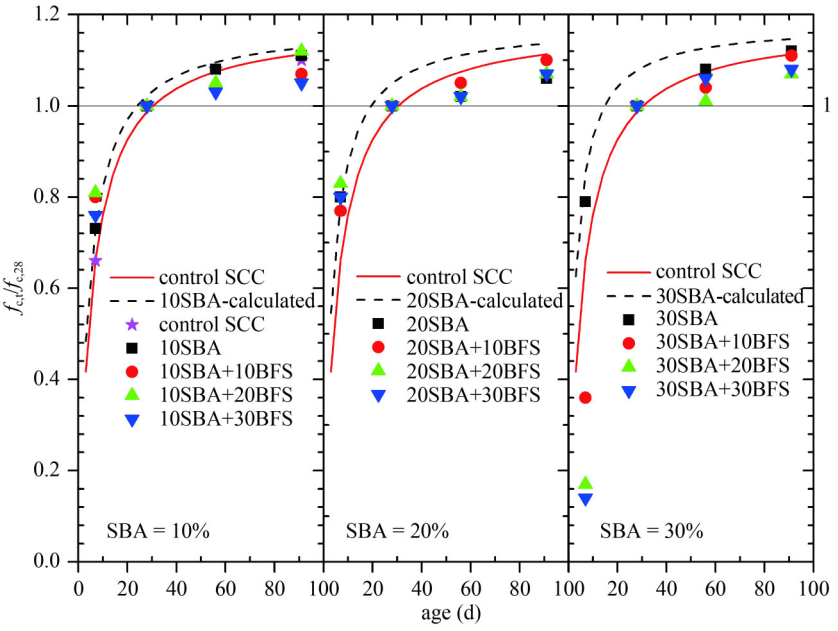

Fig. 7 Comparison of actual and calculated compressive strength evolution.

Table 9 Comparison of actual and calculated strength (MPa). Reference from Ganesan et al. [42], water-binder ratio = 0.53 (*MAPE* = 7.88%)

SBA ratio	compressive strength at different periods (MPa)									
	7 d		14 d		28 d		90 d		180 d	
	$f_{c,act.}$ ($f_{c,cal.}$)	error (%)	$f_{c,act.}$ ($f_{c,cal.}$)	error (%)	$f_{c,act.}$ ($f_{c,cal.}$)	error (%)	$f_{c,act.}$ ($f_{c,cal.}$)	error (%)	$f_{c,act.}$ ($f_{c,cal.}$)	error (%)
0.00	27.22 (24.51)	–9.96	32.3 (31.10)	–3.72	36.05 (35.9)	–0.33	38.3 (40.2)	5.06	–	–
0.05	31.11 (29.07)	–6.56	34.6 (36.42)	5.26	41.3 (41.6)	0.94	44 (46.30)	5.23	–	–
0.10	34.12 (30.72)	–9.96	40.9 (37.97)	–7.18	42.1 (43.0)	2.23	44.1 (47.4)	7.50	–	–
0.15	34.09 (31.22)	–8.43	39.9 (38.02)	–4.70	41.2 (42.6)	3.56	43.0 (46.6)	8.39	–	–
0.20	33.90 (31.34)	–7.55	37.6 (37.59)	–0.01	39.8 (41.7)	4.93	40.7 (45.2)	11.09	–	–
0.25	32.57 (27.55)	–15.42	33.1 (32.51)	–1.78	33.6 (35.7)	6.33	36.7 (38.3)	4.47	–	–
0.30	29.56 (26.34)	–10.90	30.4 (30.54)	0.47	30.8 (33.1)	7.77	31.6 (35.3)	11.72	–	–

Table 10 Comparison of actual and calculated strength (MPa). Reference from Rerkpiboon et al. [12], water-binder ratio = 0.45 (*MAPE* = 6.12%)

SBA ratio	compressive strength at different periods (MPa)									
	7 d		14 d		28 d		90 d		180 d	
	$f_{c,act.}$ ($f_{c,cal.}$)	error (%)	$f_{c,act.}$ ($f_{c,cal.}$)	error (%)	$f_{c,act.}$ ($f_{c,cal.}$)	error (%)	$f_{c,act.}$ ($f_{c,cal.}$)	error (%)	$f_{c,act.}$ ($f_{c,cal.}$)	error (%)
0.00	33.1 (27.94)	–15.58	–	–	41.1 (40.9)	–0.33	49.9 (45.8)	–8.06	51.1 (47.15)	–7.73
0.10	36.6 (33.93)	–7.29	–	–	46.5 (47.5)	2.23	54.4 (52.3)	–3.75	55.4 (53.59)	–3.27
0.20	35.2 (36.22)	2.91	–	–	46.0 (48.2)	4.93	56.6 (52.2)	–7.67	57.4 (53.25)	–7.23
0.30	33.5 (35.23)	5.17	–	–	41.2 (44.4)	7.77	51.1 (47.2)	–7.59	52.5 (47.91)	–8.74
0.40	32.7 (36.86)	12.72	–	–	39.4 (43.6)	10.77	47.7 (45.5)	–4.47	48.6 (46.03)	–5.29
0.50	28.8 (38.83)	34.82	–	–	37.6 (42.8)	13.94	45.3 (43.8)	–3.13	45.8 (44.13)	–3.65

4 Conclusions

Based on obtained results described in this study, the following remarks can be summarized.

1) SBA processed by burning at 700 °C for 1 h, and then grinding to the cement fineness (Blaine's fineness around 4000 cm^2/g) manifests pozzolanic characteristics (SAI above 80% at 7 and 28 d).

2) In fresh state, SCC mixtures incorporated with SBA or with blends of SBA and BFS results in decreasing flowability and passing ability of SCCs; whereas the flow times (via T-500 and V-funnel tests) are increased, showing more viscosity of the blended-cement composites.

3) Compressive strength of the binary-blended SCC developed with SBA is comparable or superior to that of the control SCC with pure OPC, estimated at 98%−127%. However, the joint use of SBA and BFS in ternary-blended SCCs produced a lower strength than that of the control at later ages (after 28 d). Ternary-blended SCCs containing SBA and 30% BFS (10SBA+30BFS, 20SBA+30BFS, 30SBA+30BFS) achieved strength levels of 95%−101% relative to the control after 28 d.

4) Replacement of OPC by SBA in binary-cement SCC resulted in a minor decrease in *ER* at the later ages. On the other hand, the ternary mix 10SBA+30BFS exhibited the lowest risk of corrosion after 28 d, which was a bit better than that of the control.

5) *WA* of binary-cementing specimens at later ages increases when higher amount of SBA replacement is incorporated. Meanwhile, the partial replacement of OPC by both SBA and BFS leads to reduced amount of water absorbed in the specimens, although these specimens have *WA* higher than that of the respective controls. Moreover, correlation between *WA* and *ER* can be expressed by the power formula ($ER = a \times WA^{-b}$).

6) When replacing a part of OPC by SBA or by combination of SBA and BFS, the sulfate resistance of the SCC enhances significantly. The lowest weight loss due to sulfate attack was obtained for the mix series 30SBA, followed by the mix series 20SBA and 10SBA.

7) A hyperbolic formula proposed in this study can provide a good match with the compressive strength evolution of the SBA-blended SCC. The differences between the calculated and actual strengths was estimated to be within ±10%.

Acknowledgements This research was funded by Vietnam National Foundation for Science and Technology Development (NAFOSTED) (No.107.01-2020.01).

References

1. El-Chabib H. Self-Compacting Concrete: Materials, Properties and Applications. Sawston: Woodhead Publishing, 2020: 283−308
2. Kodeboyina G B. High Performance Self-Consolidating Cementitious Composites. 1st ed. Oxford shire: Taylor & Francis, 2018
3. Subaşı S, Öztürk H, Emiroğlu M. Utilizing of waste ceramic powders as filler material in self-consolidating concrete. Construction & Building Materials, 2017, 149: 567−574
4. Sheen Y N, Le D H, Sun T H. Innovative usages of stainless steel slags in developing self-compacting concrete. Construction & Building Materials, 2015, 101: 268−276
5. Uysal M, Yilmaz K, Ipek M. The effect of mineral admixtures on mechanical properties, chloride ion permeability and impermeability of self-compacting concrete. Construction & Building Materials, 2012, 27(1): 263−270
6. Jahanzaib Khalil M, Aslam M, Ahmad S. Utilization of sugarcane bagasse ash as cement replacement for the production of sustainable concrete—A review. Construction & Building Materials, 2021, 270: 121371
7. Le D H, Sheen Y N, Lam MN T. Potential utilization of sugarcane bagasse ash for developing alkali-activated materials. Journal of Sustainable Cement-Based Materials, 2021: 1−17
8. Martirena F, Monzó J. Vegetable ashes as supplementary cementitious materials. Cement and Concrete Research, 2018, 114: 57−64
9. Figueiredo R L, Pavía S. A study of the parameters that determine the reactivity of sugarcane bagasse ashes (SCBA) for use as a binder in construction. SN Applied Sciences, 2020, 2(9): 1−15
10. Cordeiro G C, Andreão P V, Tavares L M. Pozzolanic properties of ultrafine sugar cane bagasse ash produced by controlled burning. Heliyon, 2019, 5(10): e02566
11. Jagadesh P, Ramachandramurthy A, Murugesan R. Evaluation of mechanical properties of Sugar Cane Bagasse Ash concrete. Construction & Building Materials, 2018, 176: 608−617
12. Rerkpiboon A, Tangchirapat W, Jaturapitakkul C. Strength, chloride resistance, and expansion of concretes containing ground bagasse ash. Construction & Building Materials, 2015, 101: 983−989
13. Abbas S, Sharif A, Ahmed A, Abbass W, Shaukat S. Prospective of sugarcane bagasse ash for controlling the alkali-silica reaction in concrete incorporating reactive aggregates. Structural Concrete, 2020, 21(2): 781−793
14. Joshaghani A. Concrete and Concrete Structures: A Review and Directions for Research. New York: Nova Science Publishers, Inc., 2017: 152−178
15. Bahurudeen A, Santhanam M. Influence of different processing methods on the pozzolanic performance of sugarcane bagasse ash. Cement and Concrete Composites, 2015, 56: 32−45
16. Cordeiro G C, Kurtis K E. Effect of mechanical processing on sugar cane bagasse ash pozzolanicity. Cement and Concrete Research, 2017, 97: 41−49
17. Zareei S A, Ameri F, Bahrami N. Microstructure, strength, and durability of eco-friendly concretes containing sugarcane bagasse ash. Construction & Building Materials, 2018, 184: 258−268
18. Arif E, Clark M W, Lake N. Sugar cane bagasse ash from a high-efficiency co-generation boiler as filler in concrete. Construction & Building Materials, 2017, 151: 692−703
19. ASTM C150-15. Standard Specification for Portland Cement. West Conshohocken, PA: ASTM International, 2015
20. ASTM C33-03. Standard Specification for Concrete Aggregates. West Conshohocken, PA: ASTM International, 2003
21. Chen Y Y, Tuan B L A, Hwang C L. Effect of paste amount on the properties of self-consolidating concrete containing fly ash and slag. Construction & Building Materials, 2013, 47: 340−346
22. Japan Society of Civil Engineers (JSCE). Guide to Construction of High Flowing Concrete. Tokyo: Gihoudou Pub., 1998
23. ASTM C618-08. Standard Specification for Coal Fly Ash and Raw or Calcined Natural Pozzolan for Use in Concrete. West

Conshohocken, PA: ASTM International, 2008

24. Cordeiro G C, Toledo Filho R D, Tavares L M, Fairbairn E M R. Ultrafine grinding of sugar cane bagasse ash for application as pozzolanic admixture in concrete. Cement and Concrete Research, 2009, 39(2): 110–115
25. Chusilp N, Jaturapitakkul C, Kiattikomol K. Effects of LOI of ground bagasse ash on the compressive strength and sulfate resistance of mortars. Construction & Building Materials, 2009, 23(12): 3523–3531
26. ASTM C311-05. Standard Test Methods for Sampling and Testing Fly Ash or Natural Pozzolans for Use in Portland-Cement Concrete. West Conshohocken, PA: ASTM International, 2005
27. Arenas-Piedrahita J C, Montes-García P, Mendoza-Rangel J M, López Calvo H Z, Valdez-Tamez P L, Martínez-Reyes J. Mechanical and durability properties of mortars prepared with untreated sugarcane bagasse ash and untreated fly ash. Construction & Building Materials, 2016, 105: 69–81
28. Bayapureddy Y, Muniraj K, Mutukuru M R G. Sugarcane bagasse ash as supplementary cementitious material in cement composites: Strength, durability, and microstructural analysis. Journal of the Korean Ceramic Society, 2020, 57(5): 513–519
29. Sheen Y N, Le D H, Lam M N T. Performance of self-compacting concrete with stainless steel slag versus fly ash as fillers: A comparative study. Periodica Polytechnica Civil Engineering, 2021, 65(4): 1050–1060
30. Sua-iam G, Makul N. Use of increasing amounts of bagasse ash waste to produce self-compacting concrete by adding limestone powder waste. Journal of Cleaner Production, 2013, 57: 308–319
31. Cordeiro G C, Barroso T R, Toledo Filho R D. Enhancement the properties of sugar cane bagasse ash with high carbon content by a controlled re-calcination process. KSCE Journal of Civil Engineering, 2018, 22(4): 1250–1257
32. Joshaghani A, Moeini M A. Evaluating the effects of sugarcane-bagasse ash and rice-husk ash on the mechanical and durability properties of mortar. Journal of Materials in Civil Engineering, 2018, 30(7): 04018144
33. Ríos-Parada V, Jiménez-Quero V G, Valdez-Tamez P L, Montes-García P. Characterization and use of an untreated Mexican sugarcane bagasse ash as supplementary material for the preparation of ternary concretes. Construction & Building Materials, 2017, 157: 83–95
34. International Federation for Structural Concrete (FIB). Diagnosis and Assessment of Concrete Structures—State-of-the art Report. 1989
35. Medeiros-Junior R A, Munhoz G S, Medeiros M H F. Correlations between water absorption, electrical resistivity and compressive strength of concrete with different contents of pozzolan. Revista Alconpat, 2019, 9(2): 152–166
36. Rukzon S, Chindaprasirt P. Utilization of bagasse ash in high-strength concrete. Materials & Design, 2012, 34: 45–50
37. Chi M C. Effects of sugar cane bagasse ash as a cement replacement on properties of mortars. Science and Engineering of Composite Materials, 2012, 19(3): 279–285
38. Ganesan K, Rajagopal K, Thangavel K. Evaluation of bagasse ash as supplementary cementitious material. Cement and Concrete Composites, 2007, 29(6): 515–524
39. Baroghel-Bouny V, Kinomura K, Thiery M, Moscardelli S. Easy assessment of durability indicators for service life prediction or quality control of concretes with high volumes of supplementary cementitious materials. Cement and Concrete Composites, 2011, 33(8): 832–847
40. ACI Committee 209. Prediction of Creep, Shrinkage, and Temperature Effects in Concrete Structures. Farmington Hills, MI, 1999
41. Wang C C, Wang H Y, Chen B T, Peng Y C. Study on the engineering properties and prediction models of an alkali-activated mortar material containing recycled waste glass. Construction & Building Materials, 2017, 132: 130–141
42. Ganesan K, Rajagopal K, Thangavel K. Evaluation of bagasse ash as corrosion resisting admixture for carbon steel in concrete. Anti-Corrosion Methods and Materials, 2007, 54(4): 230–236